Computational fluid dynamic investigations on a small-scale liquid sodium loop

Cite as: AIP Conference Proceedings **2445**, 020004 (2022); https://doi.org/10.1063/5.0086617
Published Online: 12 May 2022

Joachim Fuchs, Frederik Arbeiter, Michael Böttcher, et al.

Computational Fluid Dynamic Investigations on a Small-Scale Liquid Sodium Loop

Joachim Fuchs[a)], Frederik Arbeiter, Michael Böttcher, Wolfgang Hering, Heiko Neuberger, and Robert Stieglitz

Karlsruhe Institute of Technology, INR (Institute for Neutron Physics and Reactor Technology)
Hermann-von-Helmholtz-Platz 1,76344 Eggenstein-Leopoldshafen,Germany

[a)]Corresponding author: joachim.fuchs@kit.edu

Abstract. Liquid metal heat transfer systems are a technically attractive option to increase the efficiency of CSP plants. Sodium as heat transfer medium is promising especially due to high heat transfer rates. In this paper, basic considerations are made to match the requirements of a small-scale loop with sodium as heat transfer medium. The setup of the test facility KArlsruhe ReceIver test FAcility (KARIFA) to heat up this loop with a 20 kW IR laser is described. The loop is planned as an integrated design using an additive manufacturing process. Different technologies like selective laser melting (SLM) are established processes to realize an integrated design and to bring together components in one part. Some variations must be implemented to adapt these processes to liquid metal loops. The high heat fluxes also demand a flow simulation to ensure an efficient and safe operation. A Reynolds-averaged Navier-Stokes (RANS) steady state simulation was performed to show the surface and duct temperatures as well as dimensionless values to analyse the characteristics of the sodium flow.

INTRODUCTION

Several efforts to raise the temperature level and thus to enhance the efficiency of CSP plants are on the way. Among them, liquid metal heat transfer systems in CSP plants are a technically attractive option [1-3].

One of the most important properties of sodium is the high thermal conductivity that is about two orders of magnitude higher compared to molten salt. The dynamic viscosity of 0.21 $mPas^{-1}$ ensures a low pressure-loss in the loop. Sodium offers a high temperature working range from freezing (98°C) to boiling (883°C) that makes sodium an upcoming heat transfer fluid.

Another characteristic property of liquid metals is the use of electromagnetic pumps acting with magnetic induction. This enables pumping as well as flow rate measuring without active stirring parts inside the flow and without direct contact with the liquid metal [4]. Liquid metal loops offer the option of a relatively low volume of the loop due to low Prandtl numbers and properties of liquid metals in general as described above.

INSTRUMENTATION SET UP OF A SMALL-SCALE SODIUM LOOP WITHIN KARIFA PLANT

The test facility KArlsruhe ReceIver test FAcility (KARIFA) was planned to test components of CSP plants. For this purpose, a small-scale sodium loop (70 cm height) is set up to be powered by a 20 kW IR Laser (Laserline LDF 20000-200 VG64) to enable an experimental tool for investigations on sodium loops [5]. This facility consists of a 0.7 m^3 stainless steel double walled vacuum vessel with flanges for the IR Laser irradiation, for heat

SolarPACES 2020
AIP Conf. Proc. 2445, 020004-1–020004-7; https://doi.org/10.1063/5.0086617
Published by AIP Publishing. 978-0-7354-4195-8/$30.00

transfer medium supply and for cables for sensor data. The loop is currently being established using a minimized mass of sodium and an experimental set-up, that allows extreme conditions like investigations of a stagnating sodium flow.

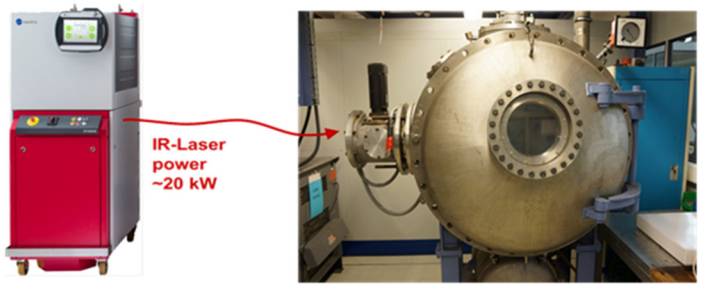

FIGURE 1. Sketch of the KARIFA basic setup

Figure 1 shows the Laser and the vessel of the KARIFA basic set-up.

In order to match the suitable energy to heat up the sodium by a laser, a pulsed mode with a broad power range is available. The equipment is just extended by a control mode of a two-colour pyrometer that allows controlling the surface temperature of the receiver surface to a defined level. Inside the vessel, an inert gas (Argon) atmosphere can be provided to the test section environment.

Basic requirements of the KARIFA plant with a small-scale sodium loop are:

- Testing of materials to investigate thermal resistance
- Design of a sodium loop for temperatures close to the boiling point
- Dynamic changes in laser input to simulate cloud course in CSP plants
- Reliability of an additive manufactured set-up for a small-scale sodium loop
- Comparison of experimental data with simulated data regarding temperatures and heat fluxes

The aim is to find a receiver design for high heat fluxes and to integrate further components like a heat exchanger in one part. Additive manufacturing processes promise to meet these requirements.

ADDITIVE MANUFACTURING PROCESSES FOR CSP COMPONENTS

In order to realize a small-scale loop with sodium as heat transfer medium, additive manufacturing was considered as a favorable process due to the option of dedicated design of functional units like receivers, sensing units and heat exchangers. This “design freedom” offers the opportunity of a seamless design, omitting welding as far as possible, thus resulting in a monolithic layout.

One suitable process for small and complex double walled parts in dimensions up to ~ 400 x 400 x 400 mm³ parts is Selective Laser Melting (SLM) [6], [7]. Examples for complex high heat flux components with similar requirements in terms of thermal loads for nuclear fusion fabricated with this powder bed process are shown in [6]-[8]. For those reasons, SLM was chosen also to manufacture a first test loop for liquid sodium in the KARIFA plant.

SLM is a powder bed process where a product is built in layers by solidification of metal powder by a laser. The production facility consists of a metal powder container that feeds the powder bed. The powder distributor wipes the powder over the building platform homogeneously. A platform is integrated that can be levelled in height and moves stepwise corresponding to the layer thickness adjusted in the process. The laser beam solidifies the powder selectively corresponding to the CAD file and thus forms the desired product slice by slice. To qualify the material properties in comparison to conventionally produced steel (e.g., rolling) in experiments performed for applications in Fusion technology, a series of pressure capsules were manufactured with 9% Cr-Steel (EUROFER). The dimensions of the capsule are 40 mm in length (connector excluded) and 20 mm in diameter, while the wall thickness is 0.8 mm (Figure 2). EUROFER steel composed mixed powder was used as powder feed material.

The capsules were leak tightness tested with Helium and finally pressurized with water until burst to determine the ultimate strength of the material. The experiment demonstrated the homogeneity of the material. The average burst pressure of all tested capsules with 0.8 mm wall thickness was 48 MPa, the variance in between the different capsules was below 10 %. The ultimate strength calculated from the recorded burst pressure was determined to ~ 600 MPa. This corresponds to > 90 % of the ultimate strength value of conventionally rolled steel in the same composition. A further result of the experiment is the observation of excessive plastic deformation of the capsule before burst. Presently studies are performed for a detailed qualification comparing the mechanical properties (strength, strain, fracture toughness, ductility, creep, and fatigue) as well as the materials' macro- and micro-structure including optimization by thermal post treatment for the 9%-Cr-steel EUROFER. Furthermore, the quantification of the difference between mixed and atomized powder from solid bars is addressed. The study is expected to be completed and published by KIT IAM in late 2020. However, the preliminary conclusion of the work is that the properties are generally very promising compared with conventionally produced material.

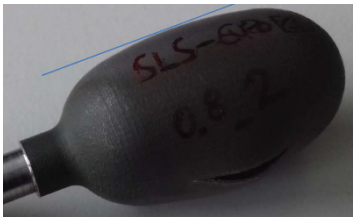

FIGURE 2. Pressure capsule as a test sample. The line in the upper part of the picture shows the plastic deformation before failure at high pressure.

The manufacturing process using metal powder as feed material however also has its limits in terms of geometries to be realized. Design rules need to be followed in order to optimize the product. The rules and guidelines to be followed in the design are well known by suppliers providing support. In addition, the orientation of a part during production is an issue to be considered in terms of geometry aspects, distortions due to thermal gradients in the powder bed but also production time and cost [8]. Qualification procedures for additive manufactured products have to include the integral powder procurement history to ensure reproducibility. Test specimen are fabricated together with products to trace the properties and to ensure a constant quality level. Manufacturers already offer powder production routines qualified by technical supervision agencies like TÜV.

BASIC CFD CALCULATIONS

To run the plant and to identify limiting parameters, it is important to find boundary conditions for the operation of the plant. To match the optimized heat transfer parameters of the operation and to reduce the number of experiments in the KARIFA plant, a series of CFD simulations is performed. This implies the variation of mass flow, sub-cooling and power impact. The aim is to identify parameters of the experimental set up that are necessary for stable and secure operation conditions in heat transfer loops. Together with experimental results, this builds the basis for the scale-up of sodium loops that go to the limit of operation conditions in terms of high heat transfer rates.

Steady state simulations were performed applying an Ω-Reynolds stress turbulence model. In case of low Prandtl number fluids such as liquid metals, the turbulent heat transfer that is usually handled by Reynolds analogy between turbulent momentum and heat transfer must be considered carefully. Usually, the ratio between eddy viscosity and turbulent thermal diffusivity – designated as turbulent Prandtl number Pr_t- is considered as constant and set to a default value of 0.85 or 0.9, which is in fact only valid for fluids with molecular Prandtl numbers Pr close to 1. This implies similar thicknesses of momentum and thermal boundary layer. In case of liquid metals with high thermal conductivity and values for $Pr<<1$, this assumption is not valid anymore. For our case, a value of 1.5 for Pr_t was used [9].

For the basic cases, 150°C was taken as inlet temperature and 0.8 m/s as average flow was set for the simulation. The heat flux at the upper receiver surface was set to 4 MW/m^2 leading to an average outlet temperature of 683°C. All other outer wall boundaries of the model are considered as adiabatic. The material properties of liquid sodium and Inconel, which is used for the solid parts, are considered as temperature dependent. Consequently, conjugate heat transfer for the solid part (indicated as pink coloured in Figure 3) is implemented in the model.

Figure 3 shows the mesh of a basic "meander design". For the presented case, the unstructured mesh contains about 4.5 million elements. In order to obtain Y^+ values close to 1, the channel walls are resolved in normal direction by a spacing of 0.005 mm for the wall closest cell layer. Y^+ is a dimensionless wall distance defined as

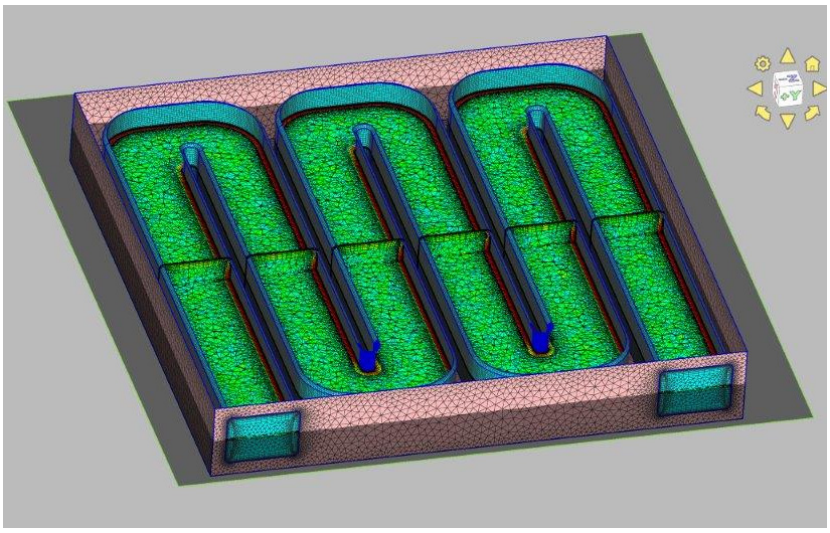

FIGURE 3. Mesh of the test receiver design. Parameters for the simulation: RANS simulation, Ω-RS turbulence model, adapted turbulent Prandtl number (1.5), temperature dependent material properties, conjugate heat transfer, adiabatic outer walls. Receiver surface area (aperture) 100x100 mm, 4 MW/m^2 heat flow, duct profile 13.73 mm x 10 mm with rounded edges (radius 1 mm), 0.8 m/s flow rate.150°C sodium inlet temperature, 683°C mean temperature outlet temperature. Material: Inconel 690, wall thickness 2.5 mm and sodium as heat transfer medium.

$y^+ = \frac{y\, u_\tau}{\nu}$, where y is the wall distance, u_τ is the wall shear velocity and ν the kinematic viscosity, see Jischa [10]. For best accuracy of heat transfer calculations the wall closest cell layer should be placed inside the viscous sublayer with a value of $y^+ < 1$, [11].

The heat flux of 4 MW/m^2 is considered as a maximum high thermal load to the receiver. For the conditions mentioned within Figure 3 the temperature of the heated surface is presented (Figure 4). The meander design shows quite low temperature gradients in areas of the duct structure but few hot spots especially at areas with high wall thickness (mainly at the edges). To avoid thermal stresses, the wall thickness could be adapted and swirl generators in the channel could reduce the local temperature maxima.

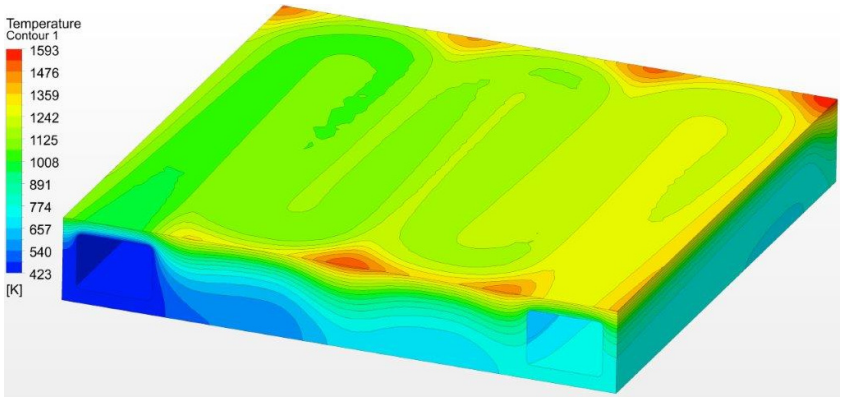

FIGURE 4. Surface temperature of the receiver design. The top surface area is irradiated by 4 MW/m^2

In order to demonstrate the temperature rise of the sodium along the duct path, two lines on the left and right side of the duct respectively (pink lines) were taken as paths to record the temperature (Figure 5).

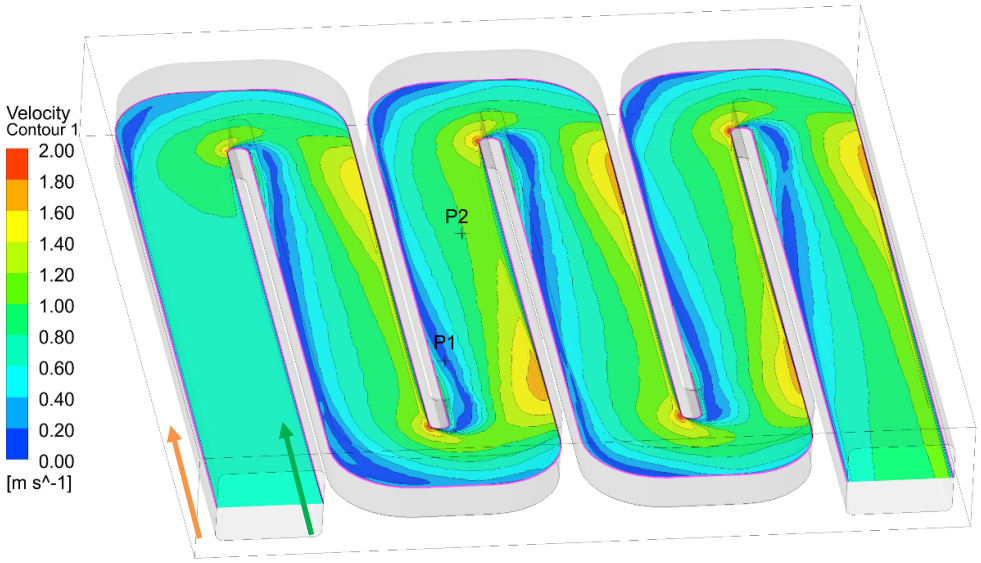

FIGURE 5. Traces along the duct to determine the temperature rise along the path length

Furthermore, the total velocity at the central channel plane is shown. In the bows the flow separates and recirculation regions are formed. The heat transfer is deteriorated leading to temperature hot spots.

Figure 6 shows the temperature rise along the paths on the wall of the duct. The development is roughly linear, with several deflections to higher temperatures. As mentioned before, this indicates flow separation and reattachment zones in the duct.

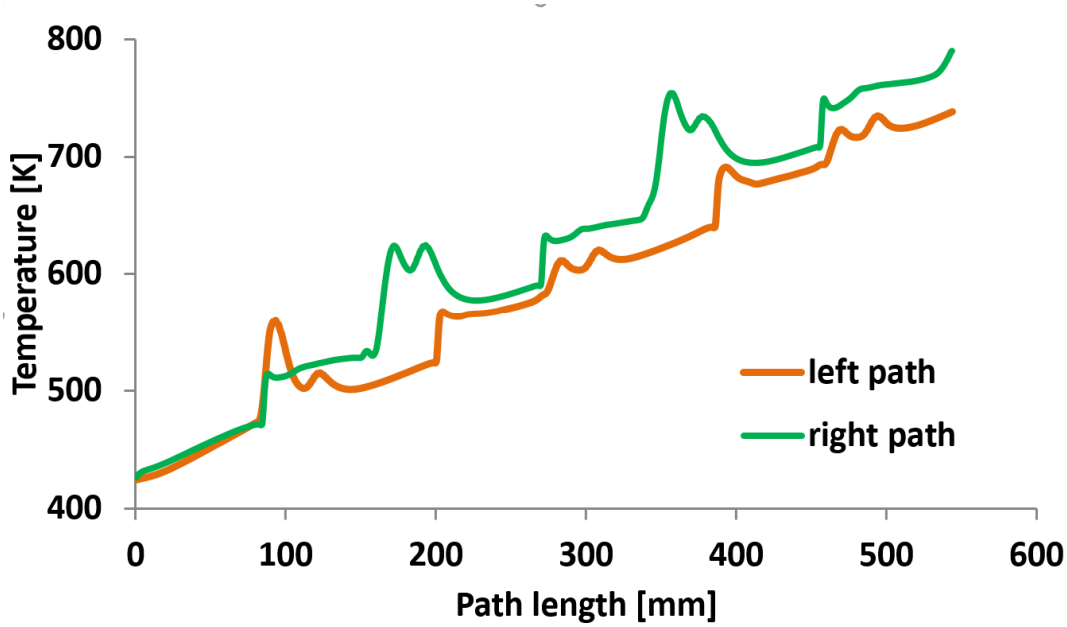

FIGURE 6. Temperature along the path length of the test receiver

As optimization parameter, the amplitude of those local hot spots should be reduced which could be achieved by implementation of swirl generators in the channel for enhanced mixing.

A study of local Nusselt numbers in dependency of the Peclet number (which is a product of the Reynolds number and the Prandtl number and commonly used for liquid metal flow) is presented by Figure 7.

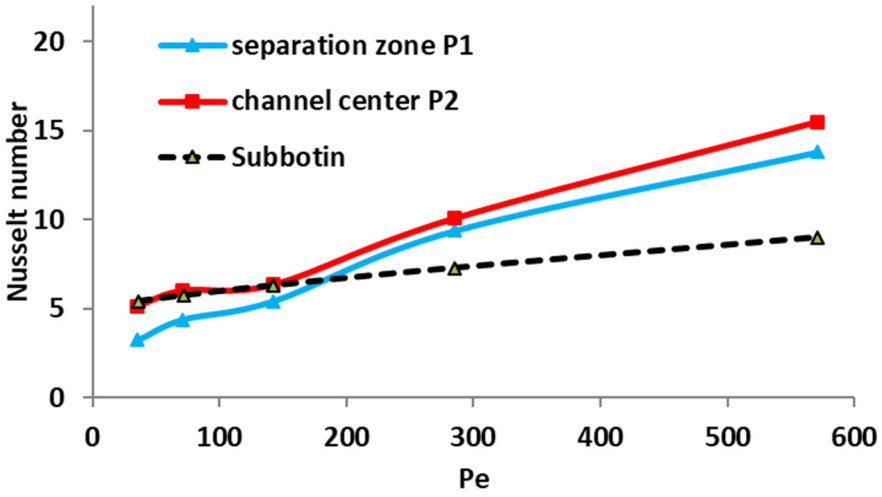

FIGURE 7. Nusselt number versus Pe-number

Position P1 is taken at the upper channel wall in the centre of a separation zone, while P2 is located at central channel position mainly not affected by separation or reattachment. An average inlet velocity of 0.8 m/s corresponds with a Peclet number of about 71. The values are compared with a correlation for uniform heated pipe flow by Subbotin [12]. As mentioned before, the local Nusselt numbers at separation zones are lower (up to 40%) for small Peclet numbers compared with those in undisturbed regions. The Nusselt numbers are higher compared to a uniformly heated pipe flow, which is a consequence of enhanced heat transfer induced by the unheated bottom of duct. The comparison is only rough because of the lack of data in literature for bottom heated channel flow. It must be mentioned that for the cases with Pe>100 the boundary layer resolution had to be refined and a wall normal spacing of 0.001 mm was used in order to keep y^+-values below 1.

CONCLUSIONS

The first results of CFD calculations show that high heat transfer rates can be utilized due to the high heat transfer values achievable with sodium. Only the thermal conductivity of Inconel 690, which is higher compared to SS316 steels, limits the heat transfer into the sodium flow, so that local hot spots were found at the bows at 4 MW/m^2.

Sodium as heat transfer medium shows excellent properties to dissipate the heat. Within a path length of about 60 cm a temperature rise of 533°C was demonstrated. Flow separation regions, furthermore temperature gradients in the solid structures leading to thermal stresses indicate a necessity of design modifications. For future work, modifications of channel wall thickness and channel geometry will be investigated. To improve heat transfer conditions and mixing additional channel wall structures will be a central point of research.

Selective laser melting is a promising manufacturing process to realize small-scale loops using an integrated design. Further SLM-specific design improvements must be implemented to realize the entire loop addressing issues like orientation, wall thickness and channel arrangement. For large-scale receivers (in the order beyond 1 meter), further options can be considered such as a modification of the SLM-production facility for continuous operation. In addition, alternative additive manufacturing processes (e.g., advanced cold spray-based deposition processes) alternated with conventional machining developed for nuclear fusion first walls could be taken into account.

ACKNOWLEDGMENTS

The authors acknowledge the financial support received from the Helmholtz Association (program “Renewable Energies”).

REFERENCES

1. Heinzel, Annette; Hering, Wolfgang; Konys, Jürgen; Marocco, Luca; Litfin, Karsten; Müller, Georg et al., "Liquid Metals as Efficient High-Temperature Heat-Transport Fluids." In: *Energy Technol.* 5.7 (2017), pp. 1026–1036. DOI: 10.1002/ente.201600721.
2. Ding, Wenjin; Shi, Hao; Jianu, Adrian; Xiu, Yanlei; Bonk, Alexander; Weisenburger, Alfons; Bauer, Thomas, "Molten chloride salts for next generation concentrated solar power plants: Mitigation strategies against corrosion of structural materials." In: *Solar Energy Materials and Solar Cells* 193 (2019), pp. 298–313. DOI: 10.1016/j.solmat.2018.12.020.
3. Onea, A.; Hering, W.; Reiser, J.; Weisenburger, A.; Diez de los Rios Ramos, N.; Lux, M. et al., "Development of high temperature liquid metal test facilities for qualification of materials and investigations of thermoelectrical modules." In: *IOP Conf. Ser.: Mater. Sci. Eng.* 228 (2017), p. 12015. DOI: 10.1088/1757-899X/228/1/012015.
4. Ratajczak, M.; Hernández, D.; Richter, T.; Otte, D.; Buchenau, D.; Krauter, N.; Wondrak, T., "Measurement techniques for liquid metals." In: *IOP Conf. Ser.: Mater. Sci. Eng.* 228 (2017), p. 12023. DOI: 10.1088/1757-899X/228/1/012023.
5. Wolfgang Hering, Alexandru Onea, Angela Jianu, Jens Reiser, Sven Ulrich, and Robert Stieglitz, "Liquid metals, materials and safety measures to progress to CSP 2.0," *SolarPaces 2018, AIP Conference Proceedings* 2126 (2019), 080002; https://doi.org/10.1063/1.5117597.
6. Neuberger, Heiko; Rey, Joerg; Arbeiter, Frederik; Hernandez, Francisco; Ruck, Sebastian; Koehly, Christina et al., "Evaluation of conservative and innovative manufacturing routes for gas cooled Test Blanket Module and Breeding Blanket First Walls." In: *Fusion Engineering and Design* 146 (2019), pp. 2140–2143. DOI: 10.1016/j.fusengdes.2019.03.124.
7. Neuberger, Heiko; Rey, Joerg; Hees, Manuel; Materna-Morris, Edeltraud; Bolich, Daniel; Aktaa, Jarir et al., "Selective Laser Sintering as Manufacturing Process for the Realization of Complex Nuclear Fusion and High Heat Flux Components." In: *Fusion Science and Technology* 72.4 (2017), pp. 667–672. DOI: 10.1080/15361055.2017.1350521.
8. H. Neuberger et al., "Advances in additive manufacturing of fusion materials," *31st Symposium on Fusion Technology* (SOFT2020).
9. Böttcher, Michael; Jäger, Wadim; Stieglitz, Robert, "KIT activities for verification and validation of liquid metals thermal hydraulics," *SESAME Workshop*, Stockholm, S, July 5-6, 2016. DOI: 10.5445/IR/1000060090.
10. Jischa, M., *Konvektiver Impuls-, Wärme- und Stoffaustausch*, Vieweg Verlag, 1982.
11. Shaw, C. T., *Using Computational Fluid Dynamics*, Prentice Hall, 1992.
12. V. I. Subbotin, P. A. Ushakov, B. N. Gabrianovich, V. D. aranov, I. P. Sviridenko, "Heat transfer to liquid metals in round tubes," *Inzhenerno-Fizicheskii Zhurnal (Journal of Engineering Physics and Thermophysics)* 6 (1963), No. 4, pp. 16-21 (in Russian).